Control of cytoplasmic and nuclear protein kinase A by phosphodiesterases and phosphatases in cardiac myocytes

Zeineb Haj Slimane, Ibrahim Bedioune, Patrick Lechêne, Audrey Varin, Florence Lefebvre, Philippe Mateo, Valérie Domergue-Dupont, Matthias Dewenter, Wito Richter, Marco Conti, et al.

Control of cytoplasmic and nuclear protein kinase A by phosphodiesterases and phosphatases in cardiac myocytes

Zeineb Haj Slimane,[1,2] Ibrahim Bedioune[1,2], Patrick Lechêne,[1,2] Audrey Varin,[1,2] Florence Lefebvre,[1,2] Philippe Mateo,[1,2] Valérie Domergue-Dupont,[2] Matthias Dewenter,[3] Wito Richter,[4] Marco Conti[4], Ali El-Armouche,[3] Jin Zhang,[5] Rodolphe Fischmeister,[1,2] Grégoire Vandecasteele[1,2]

[1]INSERM, UMR-S 769, LabEx LERMIT, DHU TORINO, F-92296, Châtenay-Malabry, France;

[2]Univ. Paris-Sud, IFR141, F-92296, Châtenay-Malabry, France;

[3]Department of Pharmacology, University Medical Center Göttingen (UMG) Heart Center, Georg August University Medical School, Göttingen, Germany;

[4]Department of Obstetrics, Gynecology, and Reproductive Sciences, Center for Reproductive Sciences, University of California, San Francisco, CA 94143, USA;

[5]Department of Pharmacology and Molecular Sciences, Johns Hopkins University School of Medicine, Baltimore, Maryland, USA.

Running title: Control of Nuclear PKA Activity in Cardiomyocytes

Correspondence to:

Grégoire Vandecasteele (e-mail: gregoire.vandecasteele@u-psud.fr)
INSERM UMR-S 769
Université Paris-Sud, Faculté de Pharmacie
5, Rue J.-B. Clément
F-92296 Châtenay-Malabry Cedex
France
Phone: +33-1-46.83.57.17
Fax 33-1-46.83.54.75

Word count: abstract + text + references + figure legends = words

Abstract

Aims The cAMP-dependent protein kinase (PKA) mediates β-adrenoceptors (β-ARs) regulation of cardiac contraction and gene expression. Whereas PKA activity is well characterized in various subcellular compartments of adult cardiomyocytes, its regulation in the nucleus remains largely unknown. The aim of the present study was to compare the modalities of PKA regulation in the cytoplasm and nucleus of cardiomyocytes.

Methods and results Cytoplasmic and nuclear cAMP and PKA activity were measured with targeted FRET probes in adult rat ventricular myocytes. β-AR stimulation with isoprenaline (Iso) led to fast cAMP elevation in both compartments, whereas PKA activity increased fast in the cytoplasm but markedly slower in the nucleus. Iso was also more potent and efficient to activate cytoplasmic than nuclear PKA. Similar slow kinetics of nuclear PKA activation was observed upon adenylyl cyclase activation with L-858051 or phosphodiesterase (PDE) inhibition with IBMX. Consistently, pulse stimulation with Iso (15 s) maximally induced PKA and myosin-binding protein C phosphorylation in the cytoplasm, but marginally activated PKA and CREB phosphorylation in the nucleus. Inhibition of PDE4 or ablation of the *Pde4d* gene in mice prolonged cytoplasmic PKA activation and enhanced nuclear PKA responses. In the cytoplasm, phosphatase 1 (PP1) and 2A (PP2A) contributed to the termination of PKA responses, whereas only PP1 played a role in the nucleus.

Conclusion Our study reveals a differential integration of cytoplasmic and nuclear PKA responses to β-AR stimulation in cardiac myocytes. This may have important implications in the physiological and pathological hypertrophic response to β-AR stimulation.

Key Words: cAMP-dependent protein kinase, compartmentation, 3'-5' cyclic nucleotide phosphodiesterases, Ser/Thr protein phosphatases, nucleus

1. Introduction

The cAMP-dependent protein kinase (PKA) is critically involved in the regulation of cardiac function by catecholamines acting on β-adrenoceptors (β-ARs) as well as several other hormonal and circulating factors acting through other G_s protein-coupled receptors (G_sPCRs). In the absence of cAMP, the PKA holoenzyme is a heterotetramer composed of two catalytic (C) subunits that are bound and inhibited by a dimer of regulatory (R) subunits. G_sPCR occupancy leads to activation of adenylyl cyclases (AC) and increase in intracellular [cAMP]. Cooperative binding of cAMP to the R subunits leads to dissociation and activation of the C subunits which phosphorylate multiple protein targets in various subcellular compartments.[1] In cardiac myocytes, the best described PKA targets are proteins involved in excitation-contraction coupling (ECC) including the sarcolemmal L-type Ca^{2+} channel, the ryanodine receptor (RyR2) and phospholamban (PLB), as well as the myofilament proteins cardiac myosin-binding protein C (cMyBP-C) and troponin I.[2]

The velocity and specificity of β-AR regulation is determined by the localization of the PKA holoenzyme to its targets by A-kinase anchoring proteins (AKAPs)[3] and by the spatiotemporal pattern of cAMP signaling, which results from the interplay between cAMP production by ACs and cAMP degradation by cyclic nucleotide phosphodiesterases (PDEs).[4] In addition, PKA activity is counterbalanced by Ser/Thr protein phosphatases (PPs).[5] In cardiac myocytes, the PDEs that degrade cAMP belong to 5 major families (PDE1-4 and PDE8) [4], whereas the major cardiac PPs are PP1, PP2A and PP2B.[5]

The development of genetically encoded indicators of cAMP levels and PKA activity has been instrumental in defining the spatiotemporal characteristics of cAMP signals and PKA activity elicited by G_sPCRs in living cardiac myocytes. The use of targeted sensors to various intracellular compartments revealed subcellular compartments with distinct cAMP responses and PKA phosphorylation gradients upon β-AR stimulation.[6,7] These studies also identified the

cAMP-specific PDE4 family as a major negative regulator of cAMP generated by β-ARs.[6] Three genes encoding PDE4 (*Pde4a, Pde4b* and *Pde4d*) are expressed in cardiac tissue, and recent studies have emphasized the importance of PDE4B and PDE4D for β-AR regulation of cardiac ECC (reviewed in [4]).

PKA regulates numerous other effectors in cardiac myocytes, notably the transcription factors belonging to the cAMP-response element binding protein (CREB) family and class II histone deacetylases (HDACs) 4 and 5 in the nucleus.[8-11] According to the classical view of nuclear PKA signaling, cAMP binds to PKA outside of the nucleus and, after dissociation from the R subunits, the C subunits cross the nuclear envelope by passive diffusion, which is a slow process.[12] However, recent evidence indicates that in HEK293 cells, a nuclear resident pool of PKA exists but is isolated from cAMP generated at the plasma membrane by AKAP-anchored PDE4.[13] In cardiac myocytes, it was reported that muscle A-kinase anchoring protein (mAKAP) targets PKA to multiple subcellular compartments including the nucleus[14] and the nuclear membrane.[15] Moreover, mAKAP binds PDE4D3, a specific PDE4 isoform, which may control cAMP levels in this compartment and thereby the release of PKA C subunits into the nucleus.[16,17] However, the modalities of nuclear PKA regulation in adult cardiomyocytes remain unknown. This issue is important given the role of the mAKAP complex and class II HDACs in the control of pathological cardiac hypertrophy[17,18] and of the CREB family of transcription factors in multiple aspects of cardiac function, including hypertrophy and apoptosis[19] as well as the deleterious effects of chronic β_1-AR overexpression in the heart.[20]

In this study, we compared the spatiotemporal dynamics of cytoplasmic and nuclear cAMP and PKA activity in adult cardiac myocytes using recombinant FRET probes targeted to these compartments. We found that upon β-AR stimulation, cAMP increases with similar fast kinetics in both compartments, whereas PKA activation is considerably delayed in the nuclei compared to the cytoplasm. Our results reveal for the first time the respective roles of PDE3

and PDE4 and of PP1, PP2A and PP2B in the differential integration of cytoplasmic and nuclear PKA responses to β-AR stimulation in cardiac myocytes.

2. Methods

All experiments performed conform to the European Community guiding principles in the care and use of animals (86/609/CEE, CE Off J no. L358, 18 December 1986), the local ethics committee (CREEA Ile-de-France Sud) guidelines, and the French decree nº 87-848 of October 19, 1987 (J Off République Française, 20 October 1987, pp 12245–12248). Authorizations to perform animal experiments according to this decree were obtained from the French Ministère de l'Agriculture, de la Pêche et de l'Alimentation (nº D 92-283, December 13, 2012). A total of 72 rats and 7 mice were used for this study.

2.1 FRET-Based Sensors of cAMP and PKA Activity

Cytoplasmic cAMP was measured using Indicator of cAMP using Epac 3 (ICUE3), a fluorescence resonance energy transfer (FRET)-based sensor.[21] Nuclear localization of ICUE3 was achieved by adding a C-terminal nuclear localization signal (ICUE3-NLS).[13] PKA activity was measured with the FRET-based A-kinase activity reporter 3 (AKAR3).[22] Because untargeted AKAR3 is localized both in the cytoplasm and the nucleus, a specific cytoplasmic localization of AKAR3 was achieved by adding a C-terminal nuclear export signal to AKAR3 (AKAR3-NES). A specific nuclear localization was obtained by adding a C-terminal nuclear localization signal (AKAR3-NLS).[22] Adenoviruses encoding Ad.AKAR3-NES and Ad.AKAR3-NLS were generated using the ViraPower Adenoviral Expression System (Invitrogen) according to the manufacturer's protocol. The adenovirus encoding ICUE3 was kindly provided by Dr. Yang K. Xiang (University of California, Davis). The adenovirus encoding ICUE3-NLS was generated by Welgen Inc.

2.2 Isolation of Adult Rat Ventricular Myocytes (ARVMs)

Male Wistar rats (200–250 g) were subjected to anaesthesia by intraperitoneal injection of pentothal (0.1 mg/g). Individual ventricular myocytes were obtained by retrograde perfusion of the hearts as previously described.[23] See Data Supplement for details.

2.3 Adenoviral Infection

The medium was replaced by 300 µL of FBS-free MEM containing one of the following adenoviruses: Ad-AKAR3-NES, Ad-AKAR3-NLS, Ad-ICUE3 or Ad-ICUE3-NLS. In some experiments, PKA was blocked by co-infecting the cells with adenoviruses encoding a rabbit muscle PKA inhibitor (Ad.PKI)[24]. All experiments were done 24-48 h after cell isolation.

2.4 FRET Measurements of Cytoplasmic and Nuclear cAMP and PKA Activity

Cells were maintained at room temperature (20-25°C) in the same Ringer solution as described above. Images were captured every 5 s using the 40x oil immersion objective of an inverted microscope (Nikon) connected to a Cool SNAP HQ2 camera (Photometrics) controlled by the Metafluor software (Molecular Devices). CFP was excited during 300 ms by a Xenon lamp (Nikon) using a 440/20BP filter and a 455LP dichroic mirror. Dual emission imaging of CFP and YFP was performed using a Dual view emission splitter equipped with a 510 LP dichroic mirror and BP filters 480/30 nm and 535/25 nm, respectively.

2.5 Western Blot Studies

ARVMs were lysed in cold HNTG buffer, proteins were resolved by SDS-PAGE, and transferred to nitrocellulose membranes. Total and phosphospecific antibodies against CREB and cMyBP-C and a calsequestrin antibody were used as detailed in the Data supplement.

2.6 Data Analysis

For FRET measurements with AKAR3-NES and ICUE3, average fluorescence intensity was measured in the entire cell or in a portion of the cytoplasm with identical results. For AKAR3-NLS and ICUE3-NLS, average fluorescence intensity was measured in a region of interest inside the nuclei. Background was subtracted and YFP intensity was corrected for CFP bleedthrough before calculating the ratio. Ratio images were obtained with ImageJ software. Average time course of the ratio represents the mean of all cells measured in a given experimental condition. The data were normalized to the ratio measured before the stimulus and expressed as percent change over basal. Student's *t*-test was used to compare two groups. Western blot data were compared with Mann-Whitney test. CRC were compared by Fisher test. p-value <0.05 was considered statistically significant. Densitometric analyses of Western blots were performed using Quantity one software (Bio-Rad).

3. Results

3.1 Real Time Measurements of Cytoplasmic and Nuclear PKA Activity in Adult Rat Ventricular Myocytes

Adenoviruses were generated to express the FRET-based A-kinase activity reporter 3 targeted to the cytoplasm (AKAR3-NES) and the nucleus (AKAR3-NLS) in ARVMs. YFP emission

images were acquired by confocal microscopy to examine their subcellular localization. As shown in Figure 1A, myocytes infected at a multiplicity of infection (MOI) of 1,000 active viral particles per cell showed AKAR3-NES expression in the cytoplasm but not in the nuclei 24 h after infection. AKAR3-NLS expression could be detected slightly earlier (18 h) in the nuclei and was excluded from the cytoplasm (Figure 1B). However, this specific localization was dependent on the time of expression and was completely lost at 48 h, unless the MOI was reduced to 200 (Supplemental Figure 1). In order to test the functionality of AKAR3 in each compartment, cells infected with Ad.AKAR3-NES or Ad.AKAR3-NLS at MOI 1,000 for 24 h were stimulated with the β-AR agonist isoprenaline (Iso, 1 µM) and the CFP and YFP fluorescence were measured simultaneously in the entire cell for AKAR3-NES and in the two nuclei for AKAR3-NLS (Figure 1C and 1D). As shown on the graphs and the corresponding pseudocolor images, Iso strongly increased the YFP/CFP ratio in the cytoplasm as well as in both nuclei. The average change was significantly larger in the cytoplasm (+38.6 ± 2.1%) than in the nuclei (+20.4 ± 2.1%, $p<0.001$) and both were abolished by application of the PKA inhibitor H89 (10 µM) or by co-expression of the PKA inhibitor peptide PKI (Figure 1E and 1F). In the absence of Iso, neither H89 nor PKI had any effect on the basal YFP/CFP ratio in the cytoplasm or in the nuclei (Supplemental Figure 2). To further characterize PKA activation by β-AR stimulation in the two compartments, concentration-response curves (CRC) to Iso were generated. Supplemental Figure 3A shows a typical experiment in a myocyte expressing AKAR3-NES and exposed to increasing concentrations of Iso between 0.1 nM and 1 µM. The YFP/CFP emission ratio increased in a concentration-dependent manner until 30 nM Iso, and the effect was fully reversible upon washout. Supplemental Figure 3B compares the average CRC obtained in the cytoplasm (black squares) and in the nucleus (white squares). Hill fit of the data yielded apparent maximal effects (E_{max}) of +46.1 ± 2.1% and +27.6 ± 6.2%, and half-maximal activation values (EC_{50}) of 1.8 ± 0.3 nM and 4.2 ± 1.0 nM in the cytoplasm and the

nuclei, respectively. The two curves were statistically different as indicated by Fisher test ($p<0.001$). When CRC to Iso were repeated in ARVMs infected with Ad.AKAR3-NES or Ad.AKAR3-NLS at MOI 1,000 during 48h and the fluorescence was measured in the entire cell, these differences were no longer observed (Supplemental Figure 4). Thus, the decreased efficiency and potency of Iso in the nucleus compared to the cytoplasm cannot be attributed to different properties of the targeted probes.

3.2 Kinetics of cAMP and PKA Activation in the Cytoplasm and in the Nucleus of Cardiac Myocytes

In addition to these steady state differences, the kinetics of PKA activation was much faster in the cytoplasm than in the nuclei upon β-AR stimulation (Figure 2A and B). Indeed, half maximal PKA activation ($t_{1/2on}$) was reached ~30 s after addition of Iso in the cytoplasm, but required ~3 min in the nuclei (Figure 2B). This difference was also observed upon direct AC activation with the hydrosoluble forskolin analogue L-858051 (L-85, 30 µM, Figure 2C and 2D) or upon global PDE blockade with IBMX (300 µM, Figure 2E and 2F). In both compartments the response to Iso was faster than the response to L-85 and to IBMX, and in the case of L-85, the maximal nuclear PKA activation (+38.8 ± 1.5%) was significantly higher than that obtained with Iso (+21.4 ± 2.4%, $p<0.001$ *versus* L-85) or IBMX (+22.1 ± 3.1%, $p<0.01$ *versus* L-85). To test whether restricted cAMP diffusion could be involved in the slow phosphorylation of AKAR3-NLS upon β-AR stimulation, we compared the kinetics of cAMP in the cytoplasm and the nuclei using the untargeted cAMP sensor ICUE3[21] and a nuclear version of the sensor, ICUE3-NLS.[13] Myocytes infected with Ad.ICUE3 and Ad.ICUE3-NLS expressed the probe in the cytoplasm and nuclei, respectively (Figure 3A). β-AR stimulation with Iso (1 µM) produced a fast increase in cAMP with similar onset kinetics ($t_{1/2on}$ ~20 s) in both compartments (Figure 3B and 3C).

In a next series of experiments, we compared the effect of a transient β-AR stimulation (Iso, 100 nM, 15 s) similar to those elicited by a startle response on cytoplasmic and nuclear PKA activities. As shown in Figure 4A, this induced a maximal activation of PKA in the cytoplasm (+49.7 ± 2.0%, P<0.001), but a marginal increase in the nuclei (+3.2 ± 0.9%, P<0.01). Similar differences were observed when comparing the PKA phosphorylation of myofilament protein cMyBP-C at Ser282 with that of the nuclear transcription factor CREB at Ser133. cMyBP-C was significantly phosphorylated upon a short (15 s) Iso stimulation (Figure 4C) while CREB was not (Figure 4D). Prolonging the Iso application to 15 min did not further increase cMyBP-C phosphorylation (Figure 4C), but significantly increased CREB phosphorylation (Figure 4D). In parallel experiments, we verified that Iso stimulation (100 nM, 15 s and 15 min) did not modify total cMyBP-C and CREB protein levels (Supplemental Figure 5). These results suggest that the PKA-dependent regulation of contractility can be dissociated from regulation of gene expression during short β-AR stimulation.

3.3 Regulation of Cytoplasmic and Nuclear PKA Activity in Cardiac Myocytes

We next sought to characterize the regulatory mechanisms governing PKA activation in the two compartments. We have shown previously that PDE3 and PDE4 account for the majority of the cAMP-hydrolyzing activity in ARVMs and that PDE4 is predominant in the degradation of cAMP generated by β-ARs at the plasma membrane and in the cytoplasm.[6] Therefore, we examined the respective contribution of these PDEs to the regulation of PKA activity in the cytoplasm and in the nuclei using the specific PDE3 inhibitor cilostamide (Cil) and the specific PDE4 inhibitor Ro 20-1724 (Ro). Neither Cil (1µM) alone nor Ro (10 µM) alone had any effect on the basal YFP/CFP ratio (Supplemental Figure 6). ARVMs overexpressing AKAR3-NES and AKAR3-NLS were briefly exposed to Iso (100 nM, 15 s) in the presence of Cil or Ro. Each inhibitor was applied during 3 minutes before the Iso pulse and continuously thereafter. As

illustrated in Figure 5, PDE3 inhibition with Cil did not alter cytoplasmic or nuclear PKA activation by Iso (Figure 5A and 5B), whereas Ro greatly prolonged PKA activation in the cytoplasm ($t_{1/2\ off}$ = 3.4 ± 0.2 min, *versus* 1.7 ± 0.1 min for Iso alone, p<0.001) and in the nuclei (Figure 5C and 5D). Because in cardiac myocytes PDE4D is enriched at the nuclear envelope,[16,17,25] we examined β-AR regulation of cytoplasmic and nuclear PKA activity in adult mouse ventricular myocytes (AMVMs) from *Pde4d*-deficient (*Pde4d*$^{-/-}$) mice.[26] In these myocytes, the response to Iso pulse stimulation in the cytoplasm was slightly but significantly prolonged compared to WT myocytes ($t_{1/2\ off}$ = 2.4 ± 0.3 min in *Pde4d*$^{-/-}$ *versus* 1.5 ± 0.2 min, in WT, p<0.05, Figure 5E). In the nuclei, similarly to what we observed in ARVMs, Iso pulse stimulation had virtually no effect on PKA activity in WT AMVMs (+1.0 ± 0.5%, p<0.01, Figure 5F). However, in *Pde4d*$^{-/-}$ myocytes, Iso stimulation increased nuclear PKA activity by ~4-fold (+3.8 ± 0.9% in *Pde4d*$^{-/-}$ *versus* WT, p<0.05, Figure 5F). These results are consistent with PDE4D being an important regulator of nuclear cAMP/PKA signalling.

3.4 Contribution of Ser/Thr Phosphatases to the Regulation of Cytoplasmic and Nuclear PKA Responses in ARVMs

In cardiac myocytes, PP1 and PP2A are the major Ser/Thr protein phosphatases that counterbalance PKA activity. To assess the contribution of these PPs to the modulation of the cytoplasmic and nuclear PKA responses, FRET experiments were performed in ARVMs expressing AKAR3-NES or AKAR3-NLS exposed to Iso pulse (100 nM, 15 s) in the presence of Calyculin A (CalyA, 100 nM), which inhibits both PP1 and PP2A. As shown in Figure 6A, CalyA markedly slowed down the dephosphorylation of AKAR3 by Iso in the cytoplasm ($t_{1/2\ off}$ =7.0 ± 1.6 min *versus* 1.5 ± 0.1 min for Iso alone, p<0.05), and unmasked a strong PKA response in the nucleus, which remained sustained for at least 8 min (Figure 6B). To determine the participation of PP2A to these effects, okadaïc acid (OA) was used at a concentration of 100

nM, at which it preferentially inhibits this phosphatase.[27] As shown in Figure 6C, OA also slowed down the dephosphorylation of AKAR3 in the cytoplasm ($t_{1/2\ off}$ =3.0 ± 0.3 min *versus* 1.5 ± 0.1 min for Iso alone, p<0.001), although to a lesser extent than CalyA (p<0.001). In contrast, OA had no effect on the nuclear PKA response to Iso pulse stimulation (Figure 6D). In another series of experiments, a potential role for PP2B (calcineurin) was investigated using the PP2B-selective inhibitor cyclosporin A (CsA, 5 µM). As shown in Figures 6E and 6F, CsA did not modify the PKA response to Iso, neither in the cytoplasm or the nucleus. Together, these results indicate that upon β-AR stimulation, PP1 and PP2A contribute to the AKAR3 dephosphorylation in the cytoplasm, whereas PP1 plays a major role in the nucleus.

4. Discussion

Although it is known that PKA can regulate cardiac gene expression through nuclear transcription factors such as CREB and specific class II HDACs, the modalities of nuclear PKA regulation have remained elusive in cardiac myocytes. Here, we show the dynamics of this regulation in response to β-AR stimulation in living adult cardiomyocytes. Our results indicate that β-AR stimulation of nuclear PKA activity is temporally dissociated from that of nuclear cAMP elevation and from that of cytoplasmic PKA activation. This is consistent with activation of the PKA holoenzyme in the cytoplasm and translocation of the C subunits to the nucleus. We show that PDE4 is an upstream negative regulator of this process, with PDE4D playing an important role to control nuclear PKA activity, whereas PP1 and PP2A are downstream negative regulators. Importantly, the contribution of PP1 and PP2A to the termination of the β-AR PKA response differs between these two compartments, with PP1 being predominant in the nucleus.

One major finding was that independently of the mechanism of cAMP elevation, the kinetics of PKA activation were much slower in the nuclei than in the cytoplasm, as previously reported in model cell lines[13,22] and primary neurons.[28] Importantly, when measuring cytoplasmic and nuclear cAMP upon β-AR stimulation, no such delay was observed (Figure 3) indicating that limited cAMP diffusion was not the cause of the slow increase in nuclear PKA activity. This was consistent with activation of PKA holoenzyme in the cytoplasm and slow translocation of the C subunits into the nuclei by passive diffusion.[12] As a result, a short β-AR stimulation marginally activated PKA and CREB phosphorylation in the nuclei while it maximally activated PKA and cMyBP-C phosphorylation in the cytoplasm (Figure 4). Such temporal dissociation of PKA action in the two compartments may have important implications for cardiac physiology and pathology. The fast kinetics of cytoplasmic PKA activation observed here closely mimic the kinetics of L-type Ca^{2+} current stimulation[6] and emphasize the importance of fast PKA activation for the velocity and efficiency of the fight-or-flight response. The modest consequences on nuclear PKA activity and CREB phosphorylation suggest that PKA regulation of cardiac contractility can be dissociated from regulation of gene expression during short term sympathetic stimulation. However, cAMP may also activate other effectors such as Epac, which was shown to be localized not only at the plasma membrane but also at the nuclear/perinuclear area in cardiomyocytes.[17,29] In adult rat ventricular myocytes, Epac activation was shown to contribute to the prohypertrophic effects of β-AR stimulation[30] in part by increasing nuclear [Ca^{2+}] and CaMKII-dependent nuclear export of HDAC5, with consequent derepression of the transcription factor MEF2.[29] Our results also show that sustained β-AR activation, as may occur during intense and prolonged physical exercise or following myocardium injury, increases nuclear PKA activity and CREB phosphorylation. While the CREB/CREM family of transcription factors may contribute to β-AR-dependent maladaptive remodelling,[19,20] PKA can also phosphorylate HDAC5 in the nucleus.[9,11] This, in

contrast to phosphorylation by CaMKII and PKD,[31-33] favours its nuclear retention, and the repression of the hypertrophic gene program.[9,11] Altogether these results illustrate the dynamic and versatile nature of nuclear cAMP signalling, which may exert both beneficial and detrimental influences on the adult heart depending on the respective balance between the different target effectors.

Our finding that PDE4 inhibition strongly prolonged β-AR stimulation of PKA activity in the cytoplasm, whereas PDE3 had no effect, is consistent with the relative contribution of these two PDE families to cAMP degradation in the cytoplasm of ARVMs following a short β-AR stimulation.[6] Analysis of cardiomyocytes from *Pde4d*$^{-/-}$ mice further show the participation of this specific isoform to termination of β-AR responses in ARVMs, which is consistent with the reported role of PDE4D in potentiating β-AR-stimulated contraction rate in neonatal cardiomyocytes from *Pde4d*$^{-/-}$ [34] and the reported roles of PDE4D variants in β-AR signalling and ECC in heart.[4,35,36] PDE3 and PDE4 represent the major PDE activities in cardiac nuclei and are primarily localised at the nuclear envelope.[25] Here we show that following short β-AR stimulation PDE4 predominates to control nuclear PKA activation. Results in cardiomyocytes from *Pde4d*$^{-/-}$ mice further indicate that the lack of PDE4D enhanced nuclear PKA responses to β-AR stimulation, which is consistent with the presence this isoform at the nuclear membrane.[16,17,25] Because at the nuclear envelope, PDE4D is integrated in a macromolecular complex including mAKAP and is involved in the regulation of cardiomyocyte hypertrophy,[17,37] our results suggest that dysregulation of nuclear PKA activity following the loss of PDE4D may participate in the late onset dilated cardiomyopathy observed in *Pde4d*$^{-/-}$ mice.[35] In HEK293 cells, PDE4 inhibition dramatically accelerated the nuclear PKA response to a maintained application of forskolin, implying that PDE4 inhibition uncovered a nuclear pool of PKA in these cells.[13] Although the pulse stimulation used here did not allow unambiguous determination of the onset kinetics, our data do not support a similar acceleration

of nuclear PKA activation by PDE4 inhibition in ARVMs (Figure 5). Rather, a different arrangement of components may exist in cardiac myocytes, with PDE4 being located at the nuclear envelope [16,25] where it controls the extent of C subunits released upon β-AR stimulation and transferred into the nucleus from an extranuclear pool of PKA holoenzyme.

Our study shows that Ser/Thr PPs PP1 and PP2A contribute differently to AKAR3 dephosphorylation between the cytoplasm and the nucleus. The balanced contribution of PP1 and PP2A in the cytoplasm is consistent with these two PPases playing a major role in controlling the phosphorylation status of ECC proteins and in counteracting the β-AR/cAMP/PKA-mediated functional effects in cardiac myocytes.[5] In contrast, PP2B inhibition had no effect, suggesting a minor participation of calcineurin in AKAR3 dephosphorylation in the bulk cytoplasm and the nuclei when PP1 and PP2A are active. A more important participation of PP2B might occur in pathological contexts such as cardiac pressure-overload hypertrophy where PP2B is activated.[38] In agreement with this hypothesis, it was reported that PP2B blunts β-AR phosphorylation of PLB in spontaneously hypertensive rats.[39] Moreover, whereas PP2B is not detected in the nuclei of normal heart, it is clearly localized in this compartment in the diseased myocardium.[40]

While our work was in revision, Yang *et al.* published an independent report in neonatal cardiomyocytes where they found similar kinetics differences in cytoplasmic and nuclear PKA activation which supports activation of the PKA holoenzyme in the cytoplasm and translocation of the C subunits to the nucleus in neonatal myocytes.[41] Yang *et al.* however did not investigate the role of PDE families in β-AR response as done here. Their modelling approach predicts a determinant role of phosphatase activity on the amplitude of nuclear PKA response, which is consistent with what we found here.

PP1 has been shown to have crucial functions in the nucleus of other cell types.[42] Our data suggest that a nuclear PP1 efficiently suppresses PKA activation in the nucleus, and this could

provide new opportunities to selectively manipulate nuclear β-AR signalling independently of ECC regulation. As stated above, it has been proposed recently that PKA favours nuclear accumulation of HDAC5, thereby inhibiting cardiomyocyte hypertrophy.[9,11] Thus, nuclear PP1 inhibition may enhance this cardioprotective effect of β-AR stimulation without increasing the phosphorylation of PLB and RyR2 as observed upon global PP1 inhibition, which ―although beneficial on the short term― is associated with an increased risk of ventricular arrhythmia and the development of a progressive cardiomyopathy with aging.[43]

In summary, our results demonstrate for the first time that β-AR stimulated PKA activity is differentially regulated in the cytoplasm and the nuclei of adult rat ventricular myocytes, and delineate the respective role of PDE3 and PDE4 and of PPs in this process. Our results unveil PP1 as a critical negative regulator of nuclear PKA in response to β-AR stimulation and this should have important functional consequences for the control of nuclear PKA targets such as the CREB family of transcription factors and class II HDACs, which are involved in pathological cardiac remodelling and in the adverse effects of chronic β-AR stimulation.

Acknowledgements

We thank Pierre Bobin, Dr. Jérôme Leroy and Dr. Martine Pomérance for helpful discussion of the data. We thank Valérie Nicolas (imaging core facility, University Paris-Sud, IFR 141) for assistance with confocal microscopy. We are also grateful to Dr. Hazel Lum (University of Illinois) for providing the adenovirus encoding PKI and to Dr. Yang K. Xiang (University of California Davis) for providing the adenovirus encoding ICUE3.

Conflict of interest: none declared

Funding

ZHS was a recipient of doctoral grants from the CORDDIM program of Région Ile-de-France and from the Fondation pour la Recherche Médicale. This work was supported by ANR grant 2010 BLAN 1139-01 (to GV), the Fondation Leducq for the Transatlantic Network of Excellence cycAMP grant 06CVD02 (to RF) and NIH grant R21HL107960 (to WR).

References

1. Tasken K, Aandahl EM. Localized effects of cAMP mediated by distinct routes of protein kinase A. *Physiol Rev* 2004;**84**:137-67.

2. Bers DM. Cardiac excitation-contraction coupling. *Nature* 2002;**415**:198-205.

3. Scott JD, Santana LF. A-kinase anchoring proteins: getting to the heart of the matter. *Circulation* 2010;**121**:1264-71.

4. Mika D, Leroy J, Vandecasteele G, Fischmeister R. PDEs create local domains of cAMP signaling. *J Mol Cell Cardiol* 2012;**52**:323-9.

5. Herzig S, Neumann J. Effects of serine/threonine protein phosphatases on ion channels in excitable membranes. *Physiol Rev* 2000;**80**:173-210.

6. Leroy J, Abi-Gerges A, Nikolaev VO, Richter W, Lechene P, Mazet JL *et al.* Spatiotemporal dynamics of beta-adrenergic cAMP signals and L-type Ca2+ channel regulation in adult rat ventricular myocytes: role of phosphodiesterases. *Circ Res* 2008;**102**:1091-100.

7. Saucerman JJ, Zhang J, Martin JC, Peng LX, Stenbit AE, Tsien RY *et al.* Systems analysis of PKA-mediated phosphorylation gradients in live cardiac myocytes. *Proc Natl Acad Sci U S A* 2006;**103**:12923-8.

8. Muller FU, Neumann J, Schmitz W . Transcriptional regulation by cAMP in the heart. *Mol Cell Biochem* 2000;**212**:11-7.

9. Ha CH, Kim JY, Zhao J, Wang W, Jhun BS, Wong C *et al.* PKA phosphorylates histone deacetylase 5 and prevents its nuclear export, leading to the inhibition of gene transcription and cardiomyocyte hypertrophy. *Proc Natl Acad Sci U S A* 2010;**107**:15467-72.

10. Backs J, Worst BC, Lehmann LH, Patrick DM, Jebessa Z, Kreusser MM *et al.* Selective repression of MEF2 activity by PKA-dependent proteolysis of HDAC4. *J Cell Biol* 2011;**195**:403-15.

11. Chang CW, Lee L, Yu D, Dao K, Bossuyt J, Bers DM. Acute beta-Adrenergic Activation Triggers Nuclear Import of Histone Deacetylase 5 and Delays Gq-induced Transcriptional Activation. *J Biol Chem* 2013;**288**:192-204.

12. Harootunian AT, Adams SR, Wen W, Meinkoth JL, Taylor SS, Tsien RY. Movement of the free catalytic subunit of cAMP-dependent protein kinase into and out of the nucleus can be explained by diffusion. *Mol Biol Cell* 1993;**4**:993-1002.

13. Sample V, Dipilato LM, Yang JH, Ni Q, Saucerman JJ, Zhang J. Regulation of nuclear PKA revealed by spatiotemporal manipulation of cyclic AMP. *Nat Chem Biol* 2012;**8**:375-82.

14. Yang J, Drazba JA, Ferguson DG, Bond M. A-kinase anchoring protein 100 (AKAP100) is localized in multiple subcellular compartments in the adult rat heart. *J Cell Biol* 1998;**142**:511-22.

15. Kapiloff MS, Jackson N, Airhart N. mAKAP and the ryanodine receptor are part of a multi-component signaling complex on the cardiomyocyte nuclear envelope. *J Cell Sci* 2001;**114**:3167-76.

16. Dodge KL, Khouangsathiene S, Kapiloff MS, Mouton R, Hill EV, Houslay MD *et al.* mAKAP assembles a protein kinase A/PDE4 phosphodiesterase cAMP signaling module. *EMBO J* 2001;**20** :1921-30.

17. Dodge-Kafka KL, Soughayer J, Pare GC, Carlisle Michel JJ, Langeberg LK, Kapiloff MS *et al.* The protein kinase A anchoring protein mAKAP coordinates two integrated cAMP effector pathways. *Nature* 2005;**437**:574-8.

18. Haberland M, Montgomery RL, Olson EN. The many roles of histone deacetylases in development and physiology: implications for disease and therapy. *Nat Rev Genet* 2009;**10**:32-42.

19. Tomita H, Nazmy M, Kajimoto K, Yehia G, Molina CA, Sadoshima J. Inducible cAMP early repressor (ICER) is a negative-feedback regulator of cardiac hypertrophy and an important mediator of cardiac myocyte apoptosis in response to beta-adrenergic receptor stimulation. *Circ Res* 2003;**93**:12-22.

20. Lewin G, Matus M, Basu A, Frebel K, Rohsbach SP, Safronenko A *et al.* Critical role of transcription factor cyclic AMP response element modulator in beta1-adrenoceptor-mediated cardiac dysfunction. *Circulation* 2009;**119**:79-88.

21. DiPilato LM, Zhang J. The role of membrane microdomains in shaping beta2-adrenergic receptor-mediated cAMP dynamics. *Mol Biosyst* 2009;**5**:832-7.

22. Allen MD, Zhang J. Subcellular dynamics of protein kinase A activity visualized by FRET-based reporters. *Biochem Biophys Res Commun* 2006;**348**:716-21.

23. Rochais F, Vandecasteele G, Lefebvre F, Lugnier C, Lum H, Mazet JL *et al.* Negative feedback exerted by cAMP-dependent protein kinase and cAMP phosphodiesterase on subsarcolemmal cAMP signals in intact cardiac myocytes: an in vivo study using adenovirus-mediated expression of CNG channels. *J Biol Chem* 2004;**279**:52095-105.

24. Lum H, Jaffe HA, Schulz IT, Masood A, RayChaudhury A, Green RD. Expression of PKA inhibitor (PKI) gene abolishes cAMP-mediated protection to endothelial barrier dysfunction. *Am J Physiol* 1999;**277**:C580-8.

25. Lugnier C, Keravis T, Le Bec A, Pauvert O, Proteau S, Rousseau E. Characterization of cyclic nucleotide phosphodiesterase isoforms associated to isolated cardiac nuclei. *Biochim Biophys Acta* 1999;**1472**:431-46.

26. Jin SL, Latour AM, Conti M. Generation of PDE4 knockout mice by gene targeting. *Methods Mol Biol* 2005;**307**:191-210.

27. Bialojan C, Takai A. Inhibitory effect of a marine-sponge toxin, okadaic acid, on protein phosphatases. Specificity and kinetics. *Biochem J* 1988;**256**:283-90.

28. Gervasi N, Hepp R, Tricoire L, Zhang J, Lambolez B, Paupardin-Tritsch D *et al.* Dynamics of protein kinase A signaling at the membrane, in the cytosol, and in the nucleus of neurons in mouse brain slices. *J Neurosci* 2007;**27**:2744-50.

29. Pereira L, Ruiz-Hurtado G, Morel E, Laurent AC, Metrich M, Dominguez-Rodriguez A *et al.* Epac enhances excitation-transcription coupling in cardiac myocytes. *J Mol Cell Cardiol* 2012;**52**:283-91.

30. Metrich M, Lucas A, Gastineau M, Samuel JL, Heymes C, Morel E *et al.* Epac mediates beta-adrenergic receptor-induced cardiomyocyte hypertrophy. *Circ Res* 2008;**102**:959-65.

31. McKinsey TA, Zhang CL, Olson EN. Activation of the myocyte enhancer factor-2 transcription factor by calcium/calmodulin-dependent protein kinase-stimulated binding of 14-3-3 to histone deacetylase 5. *Proc Natl Acad Sci U S A* 2000;**97** :14400-5.

32. Vega RB, Harrison BC, Meadows E, Roberts CR, Papst PJ, Olson EN *et al.* Protein kinases C and D mediate agonist-dependent cardiac hypertrophy through nuclear export of histone deacetylase 5. *Mol Cell Biol* 2004;**24**:8374-85.

33. Wu X, Zhang T, Bossuyt J, Li X, McKinsey TA, Dedman JR *et al.* Local InsP3-dependent perinuclear Ca2+ signaling in cardiac myocyte excitation-transcription coupling. *J Clin Invest* 2006;**116**:675-82.

34. Xiang Y, Naro F, Zoudilova M, Jin SL, Conti M, Kobilka B. Phosphodiesterase 4D is required for {beta}2 adrenoceptor subtype-specific signaling in cardiac myocytes. *Proc Natl Acad Sci U S A* 2005;**102**:909-14.

35. Lehnart SE, Wehrens XH, Reiken S, Warrier S, Belevych AE, Harvey RD *et al.* Phosphodiesterase 4D deficiency in the ryanodine-receptor complex promotes heart failure and arrhythmias. *Cell* 2005;**123**:25-35.

36. Beca S, Helli PB, Simpson JA, Zhao D, Farman GP, Jones PP *et al.* Phosphodiesterase 4D regulates baseline sarcoplasmic reticulum Ca2+ release and cardiac contractility, independently of L-type Ca2+ current. *Circ Res* 2011;**109**:1024-30.

37. Pare GC, Bauman AL, McHenry M, Michel JJ, Dodge-Kafka KL, Kapiloff MS. The mAKAP complex participates in the induction of cardiac myocyte hypertrophy by adrenergic receptor signaling. *J Cell Sci* 2005;**118**:5637-46.

38. Lim HW, De Windt LJ, Steinberg L, Taigen T, Witt SA, Kimball TR *et al.* Calcineurin

expression, activation, and function in cardiac pressure-overload hypertrophy. *Circulation* 2000;**101**:2431-7.

39. MacDonnell SM, Kubo H, Harris DM, Chen X, Berretta R, Barbe MF *et al.* Calcineurin inhibition normalizes beta-adrenergic responsiveness in the spontaneously hypertensive rat. *Am J Physiol Heart Circ Physiol* 2007;**293**:H3122-9.

40. Hallhuber M, Burkard N, Wu R, Buch MH, Engelhardt S, Hein L *et al.* Inhibition of nuclear import of calcineurin prevents myocardial hypertrophy. *Circ Res* 2006;**99**:626-35.

41. Yang JH, Polanowska-Grabowska RK, Smith JS, Shields CW 4th, Saucerman JJ. PKA catalytic subunit compartmentation regulates contractile and hypertrophic responses to beta-adrenergic signaling. *J Mol Cell Cardiol* 2013;**66C**:83-93.

42. Bollen M, Beullens M. Signaling by protein phosphatases in the nucleus. *Trends Cell Biol* 2002;**12**:138-45.

43. Wittkopper K, Fabritz L, Neef S, Ort KR, Grefe C, Unsold B *et al.* Constitutively active phosphatase inhibitor-1 improves cardiac contractility in young mice but is deleterious after catecholaminergic stress and with aging. *J Clin Invest* 2010;**120**:617-26.

Figure Legends

Figure 1. Measurements of cytoplasmic and nuclear PKA activity in ARVMs. **A and B**, Confocal YFP images of ARVMs infected with Ad.AKAR3-NES (A) and Ad.AKAR3-NLS (B). Scale bars : 10 µm. **C and D,** Time course of the normalized YFP/CFP ratio upon ß-AR stimulation by isoprenaline (Iso, 1 µM) alone and after addition of the PKA inhibitor H89 (10 µM) in myocytes expressing AKAR3-NES (C) or AKAR3-NLS (D). Pseudo-color images of the YFP/CFP ratio were recorded at the times indicated by the letters on the graphs. **E and F**, Mean variation (±S.E.M.) of the YFP/CFP ratio upon stimulation with Iso (1 µM) in the presence or absence of H89 or PKI in ARVMs expressing AKAR3-NES (E) or AKAR3-NLS (F). PKI was overexpressed by adenoviral infection. In ***E***, the numbers above the bars indicate the number of cells. In ***F***, the first number above the bars indicates the number of cells and the second indicates the number of nuclei. Data are from 8 rats. Statistical significance is indicated as ***, $p<0.001$ *versus* control; $$, $p<0.01$ *versus* Iso; $$$, $p<0.001$ *versus* Iso.

Figure 2. Comparative kinetics of cytoplasmic and nuclear PKA activation in response to different cAMP-elevating agents in ARVMs. Average time courses of the normalised YFP/CFP ratio obtained in myocytes expressing AKAR3-NES (black squares) and AKAR3-NLS (white squares) upon **A**, ß-AR stimulation with Iso (1 µM), **C**, direct adenylyl cyclase activation with L-858051 (L-85, 30 µM) and **E**, global phosphodiesterase inhibition with IBMX (300 µM). N refers to the number of cells, n refers to the number of nuclei. Each symbol on the graphs represents the mean (±S.E.M.). **B, D and F**, PKA activation kinetics ($t_{1/2on}$) obtained from experiments shown in **A, C and E**, respectively. Data are from 10 rats. Statistical significance is indicated as ***,** $p<0.001$.

Figure 3. Comparative measurements of cytoplasmic and nuclear cAMP responses to a maintained ß-AR stimulation in ARVMs. **A,** YFP images of ARVMs infected with Ad.ICUE3 or Ad.ICUE3-NLS at MOI 1,000 during 24h and 16h, respectively. **B,** Average time courses of the normalised CFP/YFP ratio during upon ß-AR stimulation with Iso (1 µM) in myocytes expressing ICUE3 (black squares) or ICUE3-NLS (white squares). Each symbol represents the mean (±S.E.M.). **C,** Kinetics of cAMP elevation ($t_{1/2on}$) obtained from experiments shown in **B.** Bar graphs represent the mean ± S.E.M. Data are from 5 rats.

Figure 4. Comparison of cytoplasmic and nuclear PKA responses upon brief β-AR stimulation in ARVMs. **A and B**, Average time course of cytoplasmic and nuclear PKA activity induced by Iso (100 nM, 15 s) in ARVMs expressing AKAR3-NES (A) and AKAR3-NLS (B). Each symbol represents the mean (±S.E.M.). **C and D**, Phosphorylation levels of cMyBP-C (C) and CREB (D) in ARVMs treated or not with 100 nM Iso for 15 seconds or 15 minutes. Calsequestrin (CSQ) was used as a loading control. Bar graphs represent the mean ± S.E.M. and the numbers above the bars indicate the number of independent experiments. Data are from 19 rats. Statistical significance between control and Iso conditions is indicated as: *, $p<0.05$; **, $p<0.01$.

Figure 5. Role of PDE3 and PDE4 in the regulation of cytoplasmic and nuclear PKA activity. **A and B,** Effect of PDE3 inhibition with 1 µM cilostamide (Cil, black squares) on cytoplasmic (A) and nuclear (B) PKA responses to Iso (100 nM, 15 s) in ARVMs expressing AKAR3-NES and AKAR3-NLS, respectively. **C and D**, Effect of PDE4 inhibition with 10 µM Ro 20-1724 (Ro, black squares) on cytoplasmic (C) and nuclear (D) PKA responses to Iso (100 nM, 15 s) in ARVMs expressing AKAR3-NES and AKAR3-NLS, respectively. Cil or Ro were applied 3 min before a 15 s pulse of Iso and then maintained throughout the experiments. Solid lines

indicate the effect of Iso alone. Data are from 4 rats. **E and F,** effect of *Pde4d* gene ablation on Iso (100 nM, 15s)-induced activation of PKA in the cytoplasm (**E**) and the nuclei (**F**) in adult mouse ventricular myocytes (AMVMs) from wild-type (WT, solid lines) and PDE4D-deficient (*Pde4d*$^{-/-}$, black squares) AMVMs. Data are from 7 mice. Each symbol in A to F represents the mean ± SEM.

Figure 6. Contribution of Ser/Thr phophatases to the apparent PKA activity in the cytoplasm and the nuclei of ARVMs. **A and B**, Effect of concomitant PP1 and PP2A inhibition with Calyculin A (CalyA, 100 nM) on cytoplasmic (A) and nuclear (B) PKA responses to Iso (100 nM, 15 s) in ARVMs. **C and D**, Effect of phosphatase 2A (PP2A) inhibition with okadaïc acid (OA, 100 nM) on Iso (100 nM, 15 s) -induced stimulation of PKA in the cytoplasm (C) and the nuclei (D) of ARVMs. **E and F**, Effect of phosphatase 2B (PP2B) inhibition with cyclosporin A (CsA, 5 µM) on transient β-AR responses in the cytoplasm (E) and the nuclei (F) of ARVMs. Cells were infected with Ad.AKAR3-NES or Ad.AKAR3-NLS for 48 h. OA (black squares), CsA (black squares), or control DMSO (solid lines) were preincubated for 1 h at 37°C and then maintained throughout the experiments. CalyA (black squares) or control DMSO (solid lines) were applied 2 minutes before the 15 s pulse of Iso and then maintained throughout the experiments. Data are from 12 rats. Each symbol in A to F represents the mean ± SEM.

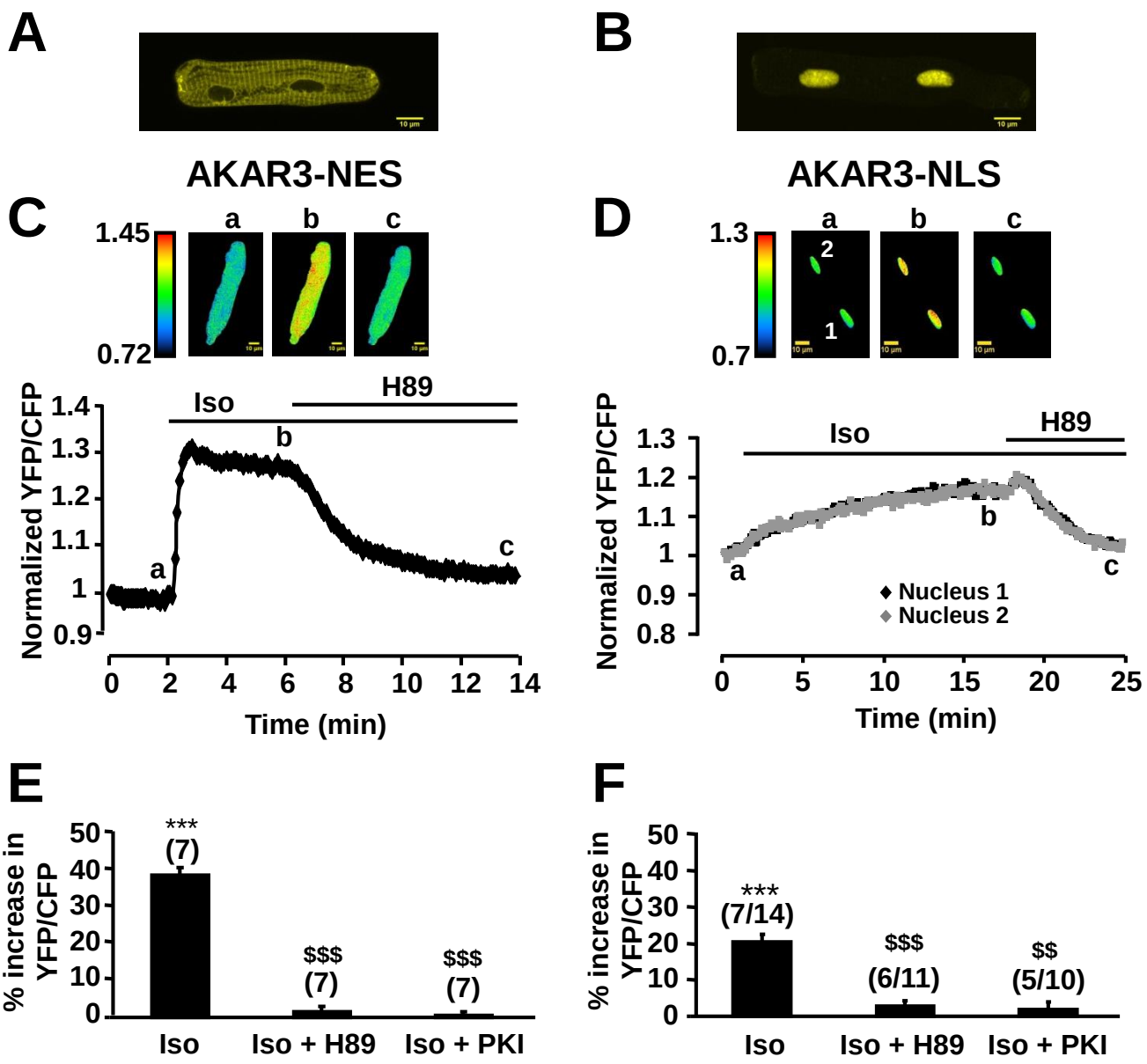
A
B
AKAR3-NES
AKAR3-NLS
C
D
1.45
0.72
1.3
0.7
a
b
c
2
1
Normalized YFP/CFP
Iso
H89
Time (min)
Nucleus 1
Nucleus 2
E
F
% increase in YFP/CFP
***
(7)
$$$
(7)
(7/14)
(6/11)
$$
(5/10)
Iso
Iso + H89
Iso + PKI

Figure 1

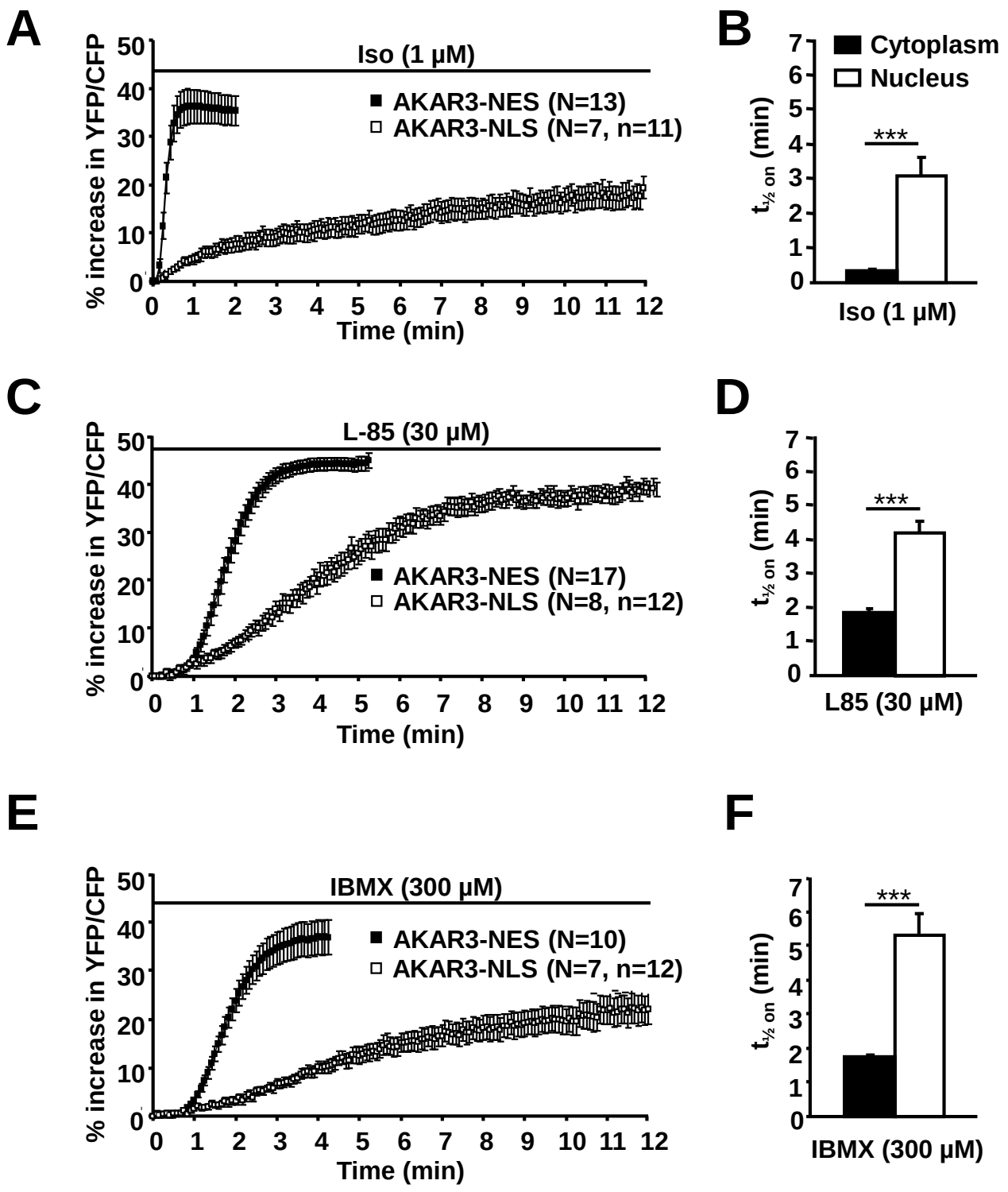
A
Iso (1 μM)
AKAR3-NES (N=13)
AKAR3-NLS (N=7, n=11)
% increase in YFP/CFP
Time (min)
B
Cytoplasm
Nucleus
***
t½ on (min)
Iso (1 μM)
C
L-85 (30 μM)
AKAR3-NES (N=17)
AKAR3-NLS (N=8, n=12)
% increase in YFP/CFP
Time (min)
D
***
t½ on (min)
L85 (30 μM)
E
IBMX (300 μM)
AKAR3-NES (N=10)
AKAR3-NLS (N=7, n=12)
% increase in YFP/CFP
Time (min)
F
***
t½ on (min)
IBMX (300 μM)

Figure 2

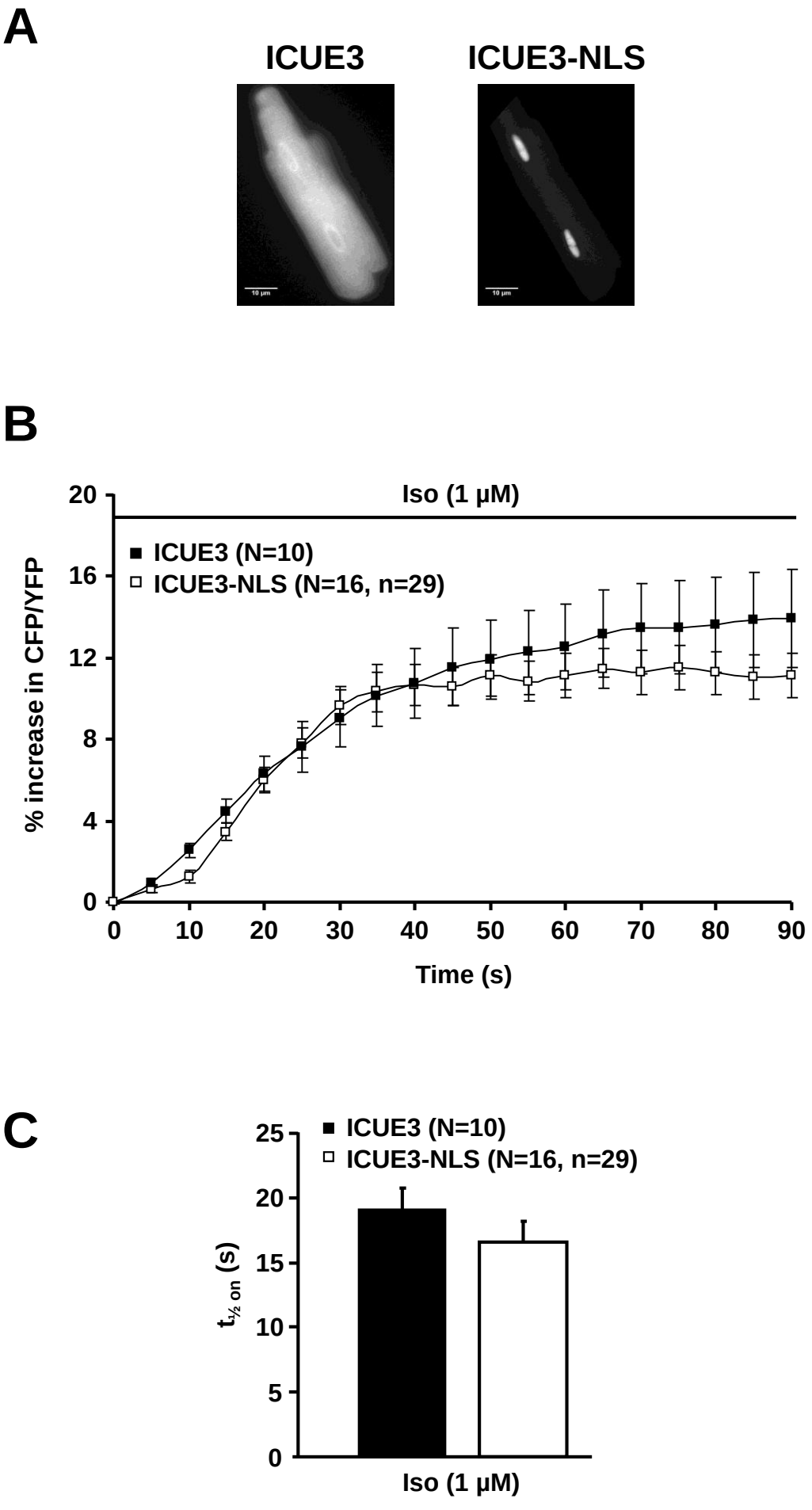
A
ICUE3
ICUE3-NLS
B
Iso (1 µM)
ICUE3 (N=10)
ICUE3-NLS (N=16, n=29)
% increase in CFP/YFP
Time (s)
C
ICUE3 (N=10)
ICUE3-NLS (N=16, n=29)
t½ on (s)
Iso (1 µM)

Figure 3

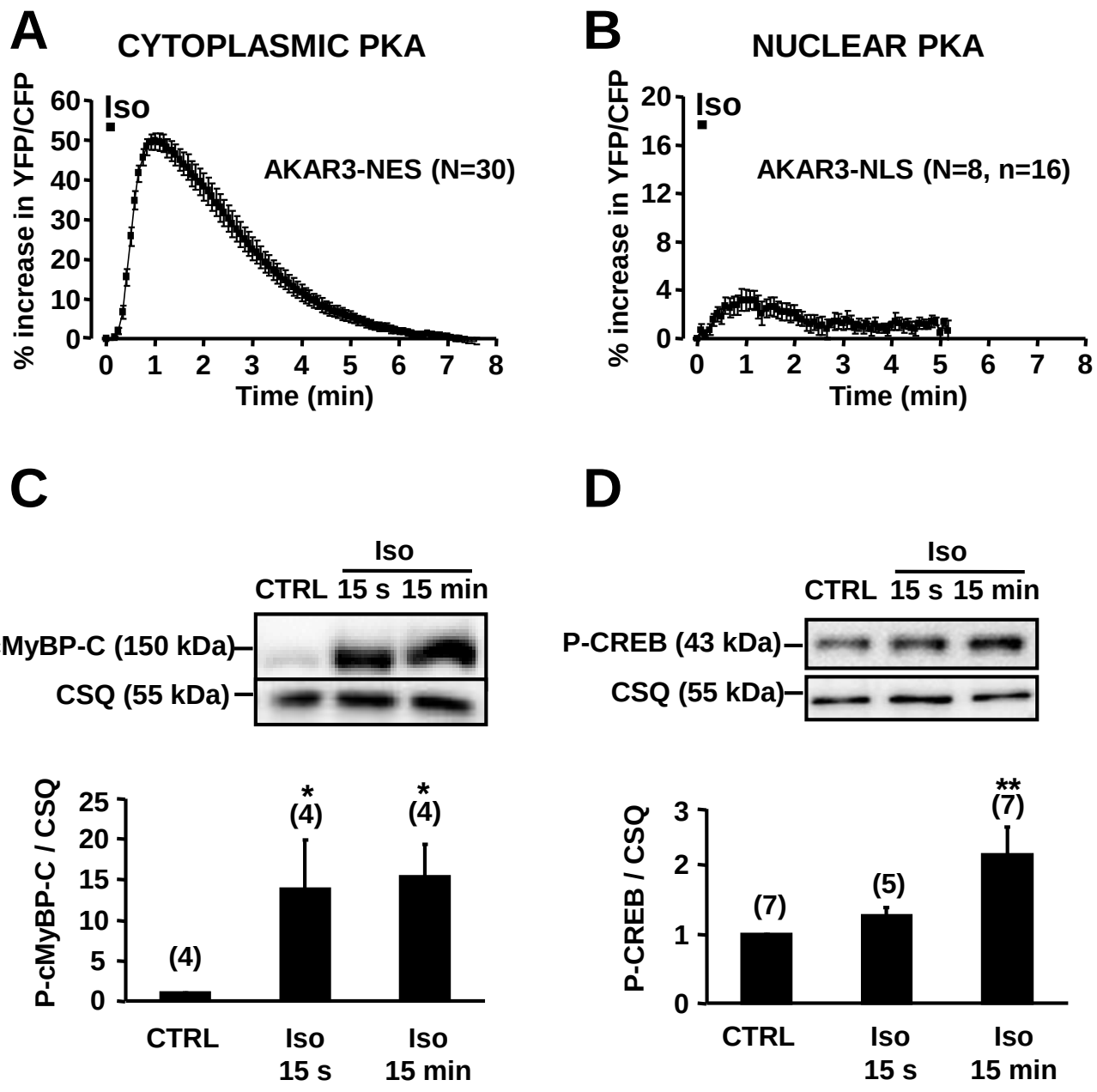
A
CYTOPLASMIC PKA
% increase in YFP/CFP
Iso
AKAR3-NES (N=30)
Time (min)
B
NUCLEAR PKA
% increase in YFP/CFP
Iso
AKAR3-NLS (N=8, n=16)
Time (min)
C
Iso
CTRL 15 s 15 min
P- cMyBP-C (150 kDa)
CSQ (55 kDa)
P-cMyBP-C / CSQ
(4)
(4)
(4)
CTRL
Iso 15 s
Iso 15 min
D
Iso
CTRL 15 s 15 min
P-CREB (43 kDa)
CSQ (55 kDa)
P-CREB / CSQ
(7)
(5)
(7)
CTRL
Iso 15 s
Iso 15 min

Figure 4

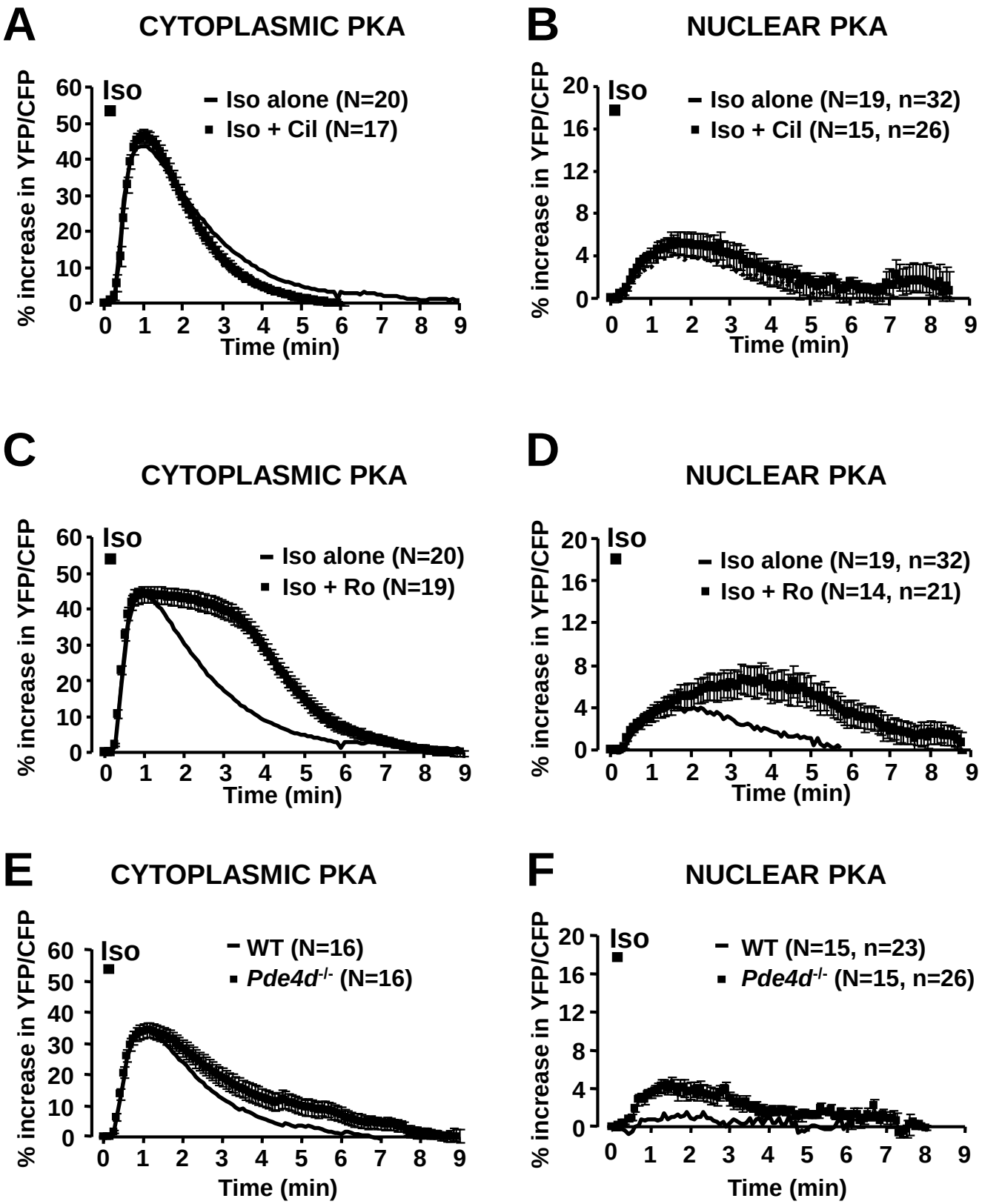
A
CYTOPLASMIC PKA
% increase in YFP/CFP
Iso
Iso alone (N=20)
Iso + Cil (N=17)
Time (min)
B
NUCLEAR PKA
% increase in YFP/CFP
Iso
Iso alone (N=19, n=32)
Iso + Cil (N=15, n=26)
Time (min)
C
CYTOPLASMIC PKA
% increase in YFP/CFP
Iso
Iso alone (N=20)
Iso + Ro (N=19)
Time (min)
D
NUCLEAR PKA
% increase in YFP/CFP
Iso
Iso alone (N=19, n=32)
Iso + Ro (N=14, n=21)
Time (min)
E
CYTOPLASMIC PKA
% increase in YFP/CFP
Iso
WT (N=16)
Pde4d-/- (N=16)
Time (min)
F
NUCLEAR PKA
% increase in YFP/CFP
Iso
WT (N=15, n=23)
Pde4d-/- (N=15, n=26)
Time (min)

Figure 5

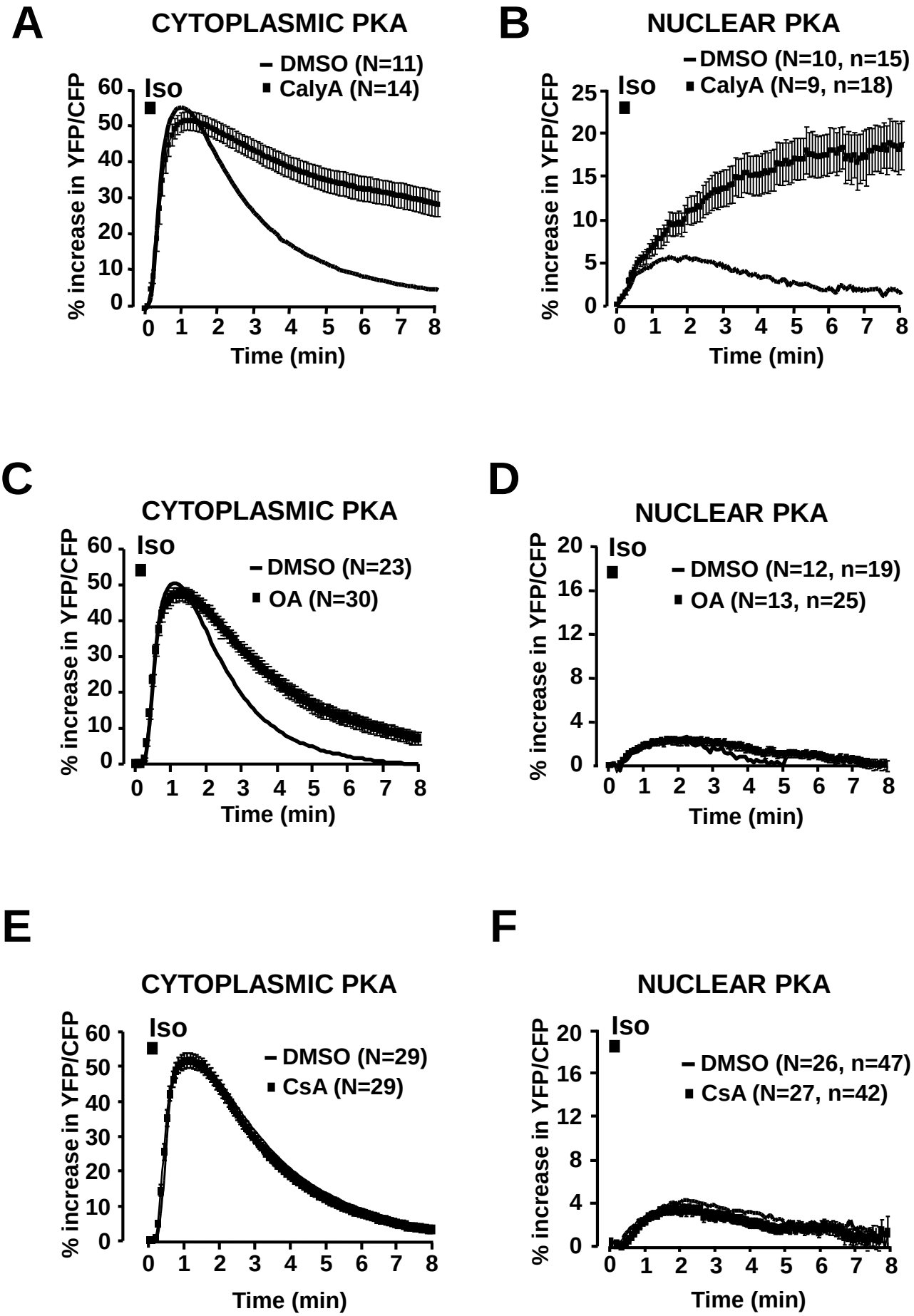
A
CYTOPLASMIC PKA
DMSO (N=11)
CalyA (N=14)
Iso
% increase in YFP/CFP
Time (min)
B
NUCLEAR PKA
DMSO (N=10, n=15)
CalyA (N=9, n=18)
Iso
% increase in YFP/CFP
Time (min)
C
CYTOPLASMIC PKA
DMSO (N=23)
OA (N=30)
Iso
% increase in YFP/CFP
Time (min)
D
NUCLEAR PKA
DMSO (N=12, n=19)
OA (N=13, n=25)
Iso
% increase in YFP/CFP
Time (min)
E
CYTOPLASMIC PKA
DMSO (N=29)
CsA (N=29)
Iso
% increase in YFP/CFP
Time (min)
F
NUCLEAR PKA
DMSO (N=26, n=47)
CsA (N=27, n=42)
Iso
% increase in YFP/CFP
Time (min)

Figure 6

Data Supplement

Control of cytoplasmic and nuclear protein kinase A by phosphodiesterases and phosphatases in cardiac myocytes

Zeineb Haj Slimane, Ibrahim Bedioune, Patrick Lechêne, Audrey Varin, Florence Lefebvre, Philippe Mateo, Valérie Domergue-Dupont, Matthias Dewenter, Wito Richter, Marco Conti, Ali El-Armouche, Jin Zhang, Rodolphe Fischmeister, Grégoire Vandecasteele

[1]INSERM, UMR-S 769, LabEx LERMIT, DHU TORINO, F-92296, Châtenay-Malabry, France;
[2]Univ. Paris-Sud, IFR141, F-92296, Châtenay-Malabry, France;
[3]Department of Pharmacology, University Medical Center Göttingen (UMG) Heart Center, Georg August University Medical School, Göttingen, Germany;
[4]Department of Obstetrics, Gynecology, and Reproductive Sciences, Center for Reproductive Sciences, University of California, San Francisco, CA 94143, USA;
[5]Department of Pharmacology and Molecular Sciences, Johns Hopkins University School of Medicine, Baltimore, Maryland, USA.

Running title: Control of Nuclear PKA Activity in Cardiomyocytes

Correspondence to:

Grégoire Vandecasteele (e-mail: gregoire.vandecasteele@u-psud.fr)
INSERM UMR-S 769
Université Paris-Sud, Faculté de Pharmacie
5, Rue J.-B. Clément
F-92296 Châtenay-Malabry Cedex
France
Phone: +33-1-46.83.57.17
Fax 33-1-46.83.54.75

Supplemental Methods

Reagents

Isoprenaline (Iso), H-89 dihydrochloride hydrate (H89), 3-isobutyl-1-methylxantine (IBMX) and Cyclosporin A (CsA) were from Sigma, L-858051 (L-85)**,** Ro 20-1724 (Ro), Okadaic Acid (OA) and Calyculin A (CalyA) were from Calbiochem, Cilostamide was from Tocris Bioscience.

Isolation of adult rat ventricular myocytes

Male Wistar rats (200–250 g) were subjected to anaesthesia by intraperitoneal injection of pentothal (0.1 mg/g), and hearts were quickly excised. Freshly isolated cells were suspended in minimal essential medium (M 4780, Sigma) containing 2.5% fetal bovine serum (FBS, PAA Laboratories), 1% penicillin-streptomycin and 2% HEPES (pH 7.6) and plated on 35 mm, laminin-coated glass bottom culture dishes for FRET experiments (10^4 cells/dish) or on 60 mm, laminin-coated culture dishes for western blot experiments ($2x10^5$ cells/dish). Myocytes were left to adhere for 2 h in a 95% O_2, 5% CO_2 incubator at 37 °C.

Isolation of adult mouse ventricular myocytes

Generation of *Pde4d*-deficient (*Pde4d*$^{-/-}$) mice has been described previously.[1] Three to six month-old wild type (WT) and *Pde4d*$^{-/-}$ males with a mixed 129/Ola (25%) and C57BL/6 (75%) background were anesthetized by intraperitoneal injection of pentothal (0.15 mg/g), and hearts were quickly removed. Ventricular myocytes were obtained by retrograde Langendorff perfusion of the heart as previously described.[2] Freshly isolated ventricular myocytes were suspended in MEM (Gibco 51200) supplemented with 5% FBS, 2% penicillin-streptomycin, 0.1% BSA, 2 mM L-glutamine, 10 mM BDM and Insulin Transferin

Selenium 1X and plated on 35 mm culture dishes coated with laminin (10 µg/ml) at a density of 10^4 cells per dish. The cells were left to adhere for 2h at 37°C.

Localisation of AKAR3-NES and AKAR3-NLS by Confocal Microscopy

Images were acquired with a Zeiss LSM 510 confocal microscope using a Plan-Apochromat 63x/1.4 oil-immersion objective. Cells were bathed in a Ringer solution containing (in mM): NaCl 121.6, KCl 5.4, $MgCl_2$ 1.8, $CaCl_2$ 1.8, $NaHCO_3$ 4, NaH_2PO_4 0.8, D-glucose 5, sodium pyruvate 5, HEPES 10 (pH 7.4), at room temperature (20-25°C), and YFP was excited using the 488 nm line of an argon laser. Emitted light was filtered with emission filter LP 530 nm.

Cell stimulation for Western Blot studies

ARVMs were incubated in FBS-free MEM containing 100 nM isoprenaline (Iso) for 15 seconds or 15 minutes. Stimulation was stopped by fast exchange of the Iso-containing medium with 2 mL of cold PBS (PAA Laboratories).

Western Blot studies

ARVMs were lysed in cold HNTG lysis buffer containing (in mM): Hepes (pH 7.5) 50; NaCl 400; Na-pyrophosphate 10; $MgCl_2$ 1.5; EGTA 1; Glycerol 10%, Triton X100 1% supplemented with phosphatase inhibitor cocktail (Roche) and a protease inhibitor cocktail (Roche). The lysates were centrifuged at 13,000g and proteins were resolved by SDS-PAGE, and transferred to nitrocellulose membranes. The membranes were saturated with 3% BSA and incubated overnight at 4°C with phosphospecific antibodies against CREB (Ser133, Cell Signaling Technology) and cMyBP-C (Ser282, Alexis). Immunoreactive proteins were revealed using anti-rabbit IgG conjugated with horseradish peroxidase (Santa Cruz). The membranes were stripped with Reblot plus Strong solution (Millipore) and reprobed with a

calsequestrin antibody (Affinity BioReagents) used as a loading control or MyBPC3 (K-16) against total cMyBP-C (Santa Cruz). Total CREB was detected with 48H2 antibody (Cell Signaling Techonology).

Supplemental References

1. Jin SL, Latour AM, Conti M. Generation of PDE4 knockout mice by gene targeting. 2005;**307**:191-210

2. Leroy J, Richter W, Mika D, Castro LR, Abi-Gerges A, Xie M, Scheitrum C, Lefebvre F, Schittl J, Mateo P, Westenbroek R, Catterall WA, Charpentier F, Conti M, Fischmeister R, Vandecasteele G. Phosphodiesterase 4B in the cardiac L-type Ca2+ channel complex regulates Ca2+ current and protects against ventricular arrhythmias in mice. 2011;**121**:2651-61

Supplemental Figures

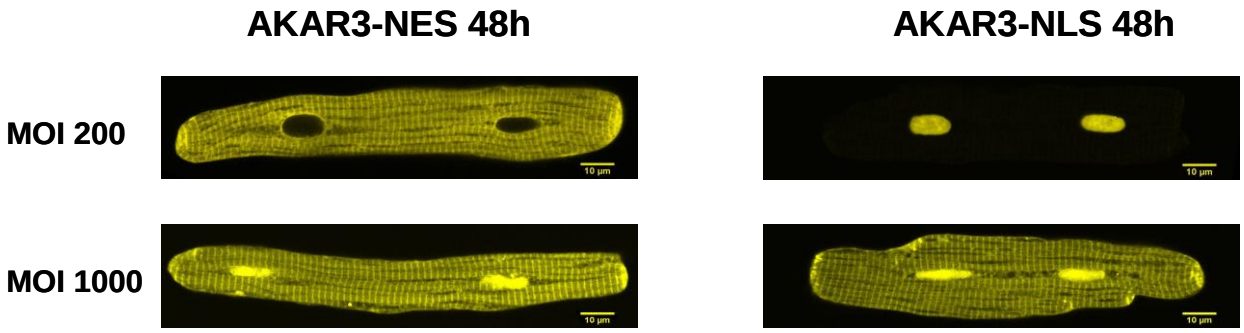

Supplemental Figure 1: Subcellular localization of AKAR3-NES and AKAR3-NLS in ARVMs depends on expression level. YFP images of ARVMs infected with Ad.AKAR3-NES and Ad.AKAR3-NLS at MOI 200 or MOI 1000 for 48h obtained by confocal microscopy. Scale bars represent 10 µm.

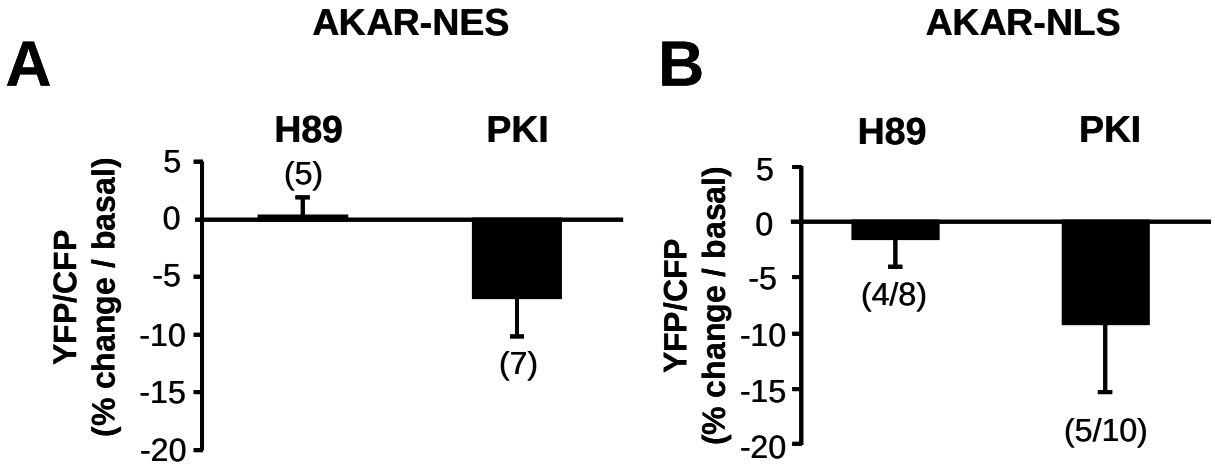

Supplemental Figure 2: PKA inhibition with H89 or PKI has no significant effect on the basal FRET ratio measured with AKAR-NES in the cytoplasm and AKAR-NLS in the nucleus. Mean variation (±S.E.M.) of the basal YFP/CFP ratio induced by H89 (10 µM) in ARVMs expressing AKAR-NES (***A***) or AKAR-NLS (***B***). PKI was co-expressed with the FRET sensors by adenoviral infection, and the mean variation (±S.E.M.) in YFP/CFP ratio were compared to cells expressing AKAR-NES alone or AKAR-NLS alone (n=7 cells each). For AKAR-NES, the numbers next to the bars indicate the number of cells. For AKAR-NLS, the first number below the bars indicates the number of cells and the second indicates the number of nuclei. Data are from 5 rats.

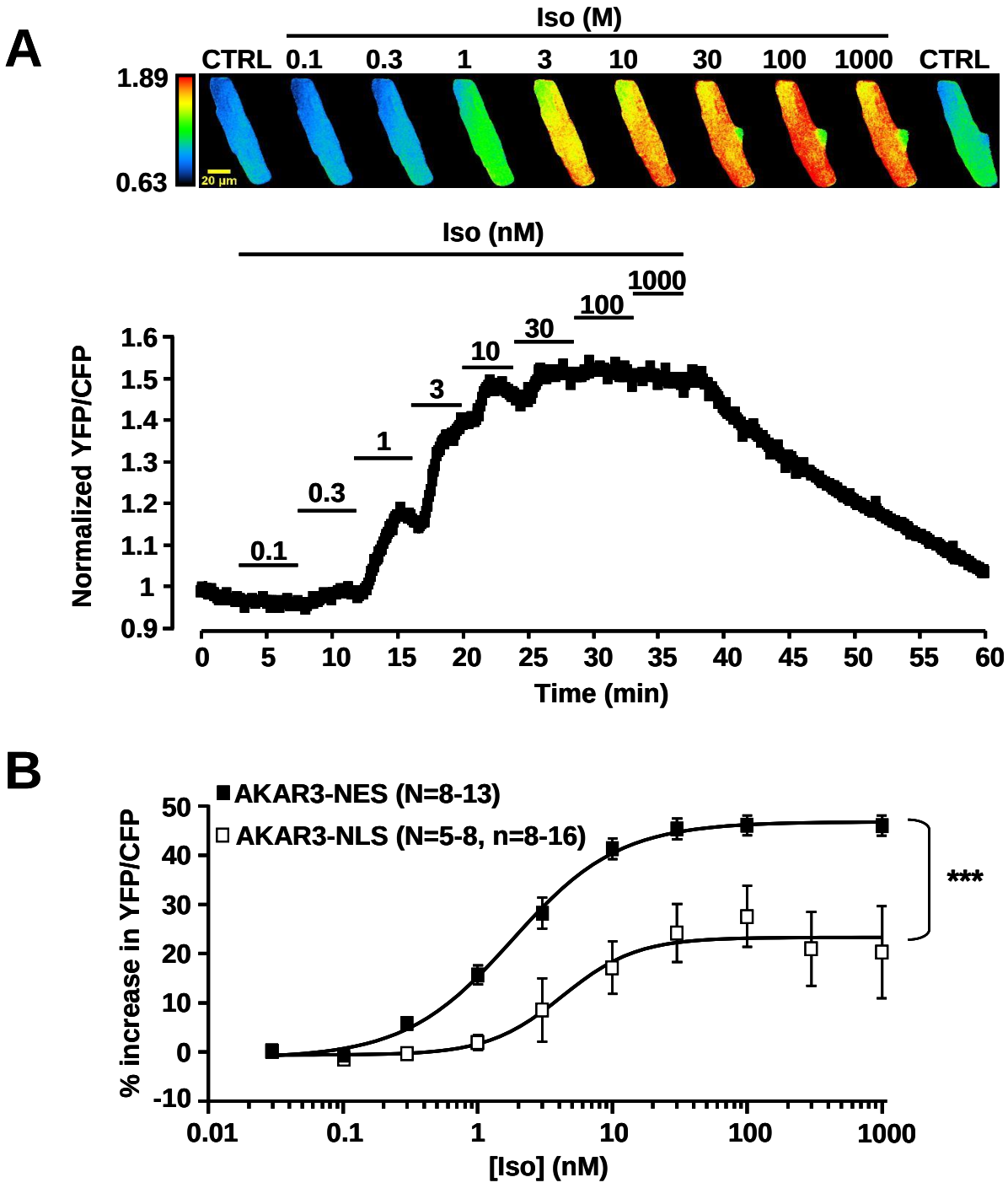

Supplemental Figure 3. Cumulative concentration-response curves (CRCs) of cytoplasmic and nuclear PKA activity in response to Iso in ARVMs. A, Time course of the normalized YFP/CFP ratio in response to increasing concentrations of Iso in a myocyte expressing AKAR3-NES. Pseudo-color images depict the variations of the YFP/CFP emission ratio at each Iso concentration. B, Comparison of the average effect of Iso on cytoplasmic (black squares) and nuclear (white squares) PKA activity. N refers to the number of cells, n refers to the number of nuclei. Data are from 6 rats. The curves were fitted with the Hill equation. Values are means ± S.E.M. Statistical significance is indicated as ***, $p<0.001$.

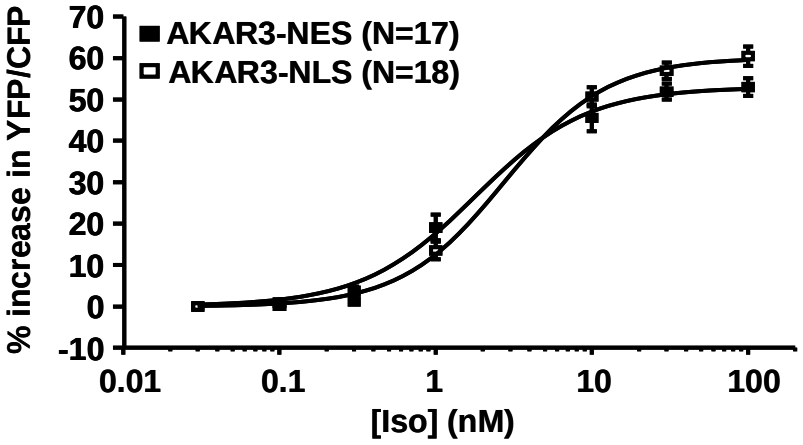

Supplemental Figure 4: Loss of the specific subcellular localization of AKAR3-NES and AKAR3-NLS yields identical CRC to Iso in ARVMs. Comparison of the average PKA activation to increasing concentrations of Iso in ARVMs infected with Ad.AKAR3-NES (black squares) or Ad.AKAR3-NLS (white squares) at MOI 1000 for 48h. Measurements were performed on the entire cell. Symbols indicate mean (±S.E.M.) and the solid lines are Hill fit of the data. E_{max} were +52.9±2.1% and +60.5±2.4% and EC_{50} were 1.7±0.2 nM and 2.6±0.3 nM for AKAR3-NES and AKAR-NLS, respectively. Data are from 2 rats.

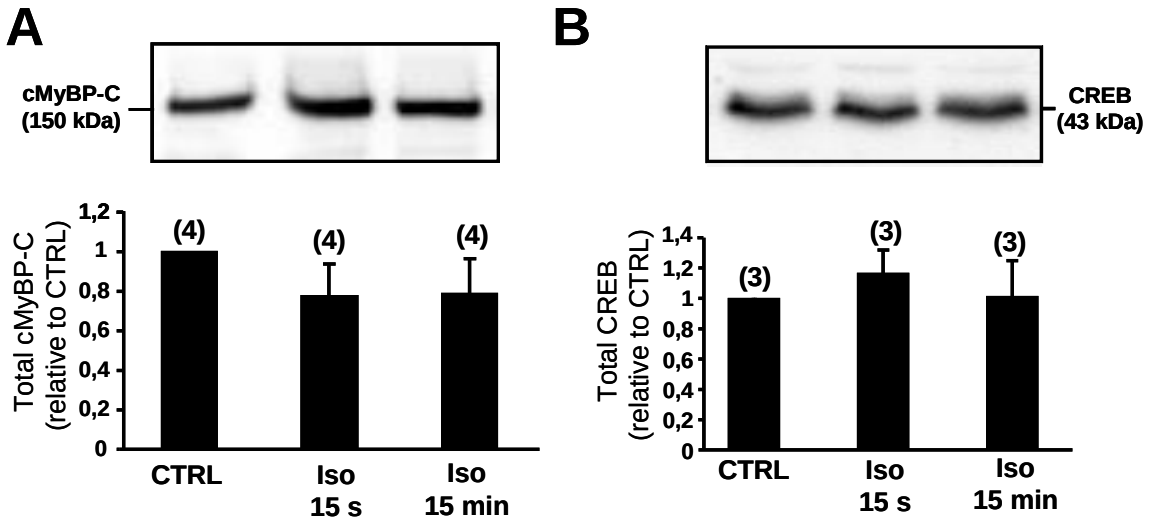

Supplemental Figure 5: β-AR stimulation with Iso (100 nM, 15 s and 15 min) does not modify total protein levels of cMyBP-C and CREB in ARVMs. ***A***, membranes from experiments in Figure 4C were stripped and probed with an antibody against total cMyBP-C. ***B***, in the case of CREB the same operation did not yield sufficient signal so datas come from 3 additional experiments. Data are from 7 rats.

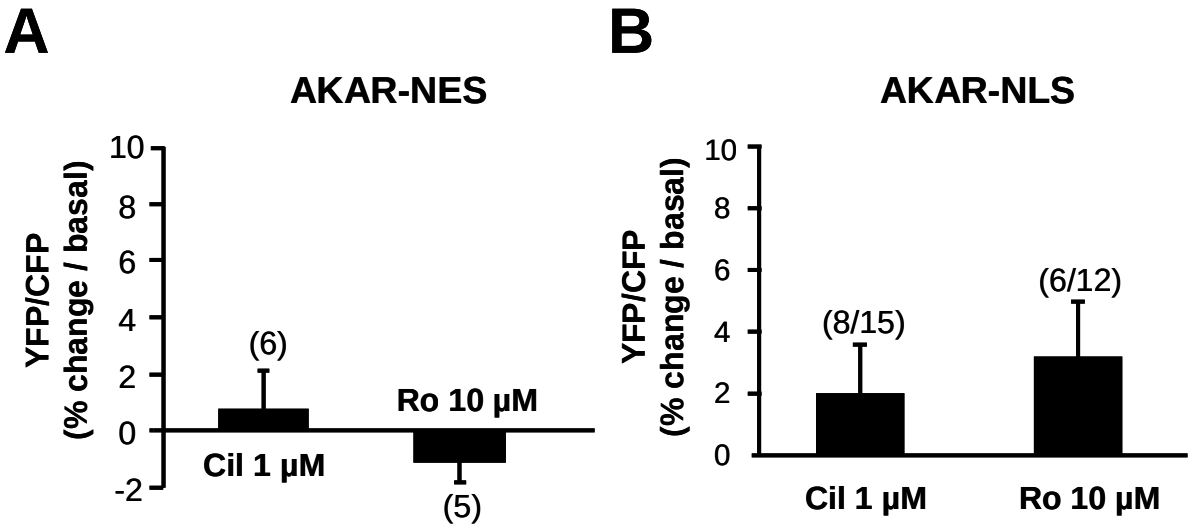

Supplemental Figure 6: Inhibition of PDE3 or inhibition of PDE4 have no significant effect on the basal FRET ratio measured with AKAR-NES in the cytoplasm and AKAR-NLS in the nucleus. Mean variation (±S.E.M.) of the basal YFP/CFP ratio induced by the PDE3 inhibitor cilostamide (Cil) and the PDE4 inhibitor Ro 20-1724 (Ro) in ARVMs expressing AKAR-NES (***A***) or AKAR-NLS (***B***). For AKAR-NES, the numbers next to the bars indicate the number of cells tested. For AKAR-NLS, the first number indicates the number of cells and the second indicates the number of nuclei. Data are from 2 rats.